Laurent, D., et al., 2023, Unravelling biotic versus abiotic processes in the development of large sulfuric-acid karsts: Geology, https://doi.org/10.1130/G50658.1

SUPPLEMENTAL MATERIAL

Unravelling biotic vs. abiotic processes in the development of large sulfuric acid karsts

D. Laurent, G. Barré, C. Durlet, P. Cartigny, C. Carpentier, G. Paris, P. Collon, J. Pironon, E.C. Gaucher

This file contains additional elements concerning (i) the extended description of the data and methods, (ii) the data table of isotopic analyses, (iii) details on the CO_2 budget calculation, and (iv) additional references.

1. Extended description of data and methods

1.1. Observations and mineralogy

Observation of thin sections was made using an Olympus BX51 optical microscope, with reflected and transmitted light, and coupled with a high resolution camera Zeiss Axiocam Icc 3M pixels.

10 cave sulfate samples have been analysed on powder using Diffuse Reflectance Infrared Fourier Transform (DRIFT) spectroscopy and X-Ray Diffraction (XRD). DRIFT and XRD measurements were carried out respectively at the GeoRessources Laboratory and CRM2 Laboratory at the University of Lorraine (Nancy, France). DRIFT spectra were recorded in the mid-infrared range with a spectral resolution of 2 cm^{-1} using a Fourier transform infrared spectrometer (BRUKER IFS 55). The spectrometer is equipped with a large-band mercury cadmium telluride (MCT) detector cooled at 77 K and associated with a diffuse reflectance attachment (Harrick Corporation). The dry samples were analysed with a dilution of 15% by weight in potassium bromide (KBr), used as a reference. XRD analyses were made using a Bruker D2 phaser with a SSD160 detector. Results were collected over the range of 2-3 to 70-75° 2θ using a step interval of 0.02°2θ every 0.6s. For both methods, obtained spectra were compared to reference bibliotheca to identify the exact nature of sulfate minerals.

1.2. In-situ gas analyses by the analyser GA5000

The methodology consists in drilling a hole within the rock, around 20 cm-long and 16 mm in diameter, and in analysing the gas composition using a GA5000 gas analyser (®Geotech) directly after the hole generation. Analyses were performed in several outcrops to target the location of the H_2S-rich carbonate rocks (see Fig.1a for location of measurements). This technique allows to detect a H_2S concentration up to 200 ppmv released from the rock. Error is

estimated to be 2% of the full-scale value obtained for the analysed gas.

*1.3.*Multiple sulfur isotopy

Sampling of the sulfur-rich minerals and karstic springs

Sulfur isotope analyses were used to identify the source of cave sulfate minerals. In addition to the sulfate minerals sampled in both the Nébélé and Azaleguy caves, samples representing all possible sources of sulfur across the Arbailles basin were also collected:

- Nébélé Cave sulfate minerals: gypsum in the Scrouitch gallery (NEB01, 02, 03, 04), thenardite/mirabilite in the Scrouitch gallery (NEB05, 06, 07, 08) (see sample location in Supplementary Fig.1);
- gypsum (n=6) in the Azaleguy Cave (AZA01 to 06; Supplementary Fig.2);
- sulfur species contained within the Nébélé Cave host rock (Dogger carbonate): H_2S evidenced by *in-situ* gas analyses within the carbonate rock (NEBe1- Fig.1a in the main text; NEBn1, n2, n3; Supplementary Fig.1). In addition, a down-rock profile of trace sulfate minerals was made in the host rock (samples NEBt; Supplementary Fig.1 for sample location), which is in contact with cave gypsum at 2 mm, 1 cm and 3 cm from the gypsum-carbonate interface (Supplementary Fig.3). The aim was to track a potential invasion of sulfuric acid during the dissolution of the host carbonate;
- disseminated sulfides (pyrites and pyrrhotites) in Liassic and Cretaceous carbonate strata (see location on Fig.1a in the main text). Sulfides are absent in the Hosta marls and Ste Suzanne marls;
- dissolved H_2S and sulfate ions from three strategic spring waters: the resurgence of the Nebele Cave (Uthurbietta spring), the Camou hot spring, and the H_2S-rich spring of Mainaltea (see locations in Fig.1a of the main text);
- Triassic evaporitic gypsum sampled at the Caresse Quarry (South Aquitaine basin, 40 km north of the Nébélé Cave).

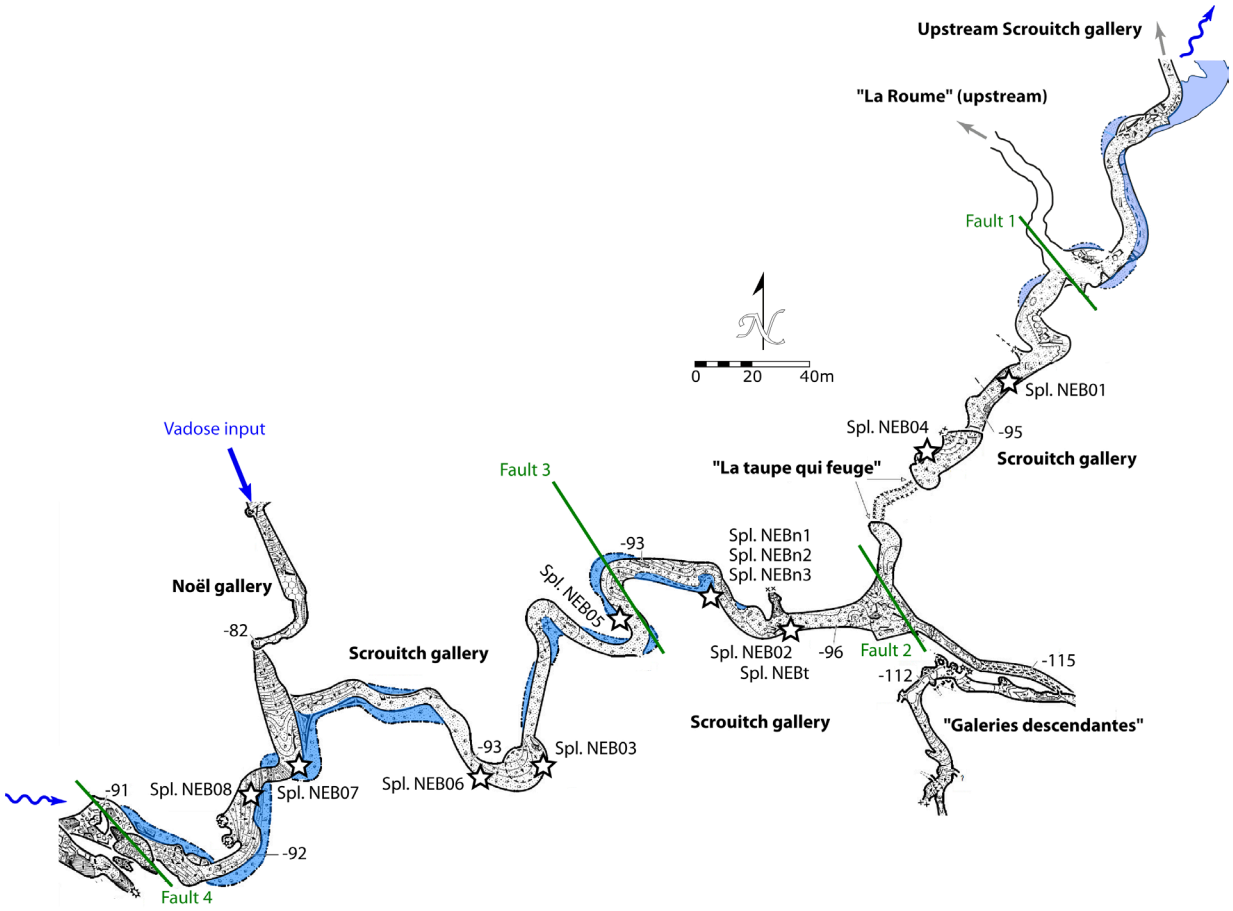

Figure S1: Detailed topography of the Scrouitch gallery (modified, provided by the "Collectif Nébélé") with position of host rock and speleothems samples. Lateral dissolution notches are highlighted in light blue. The negative numbers corresponds to the altimetry in meter relative to the cave entrance.

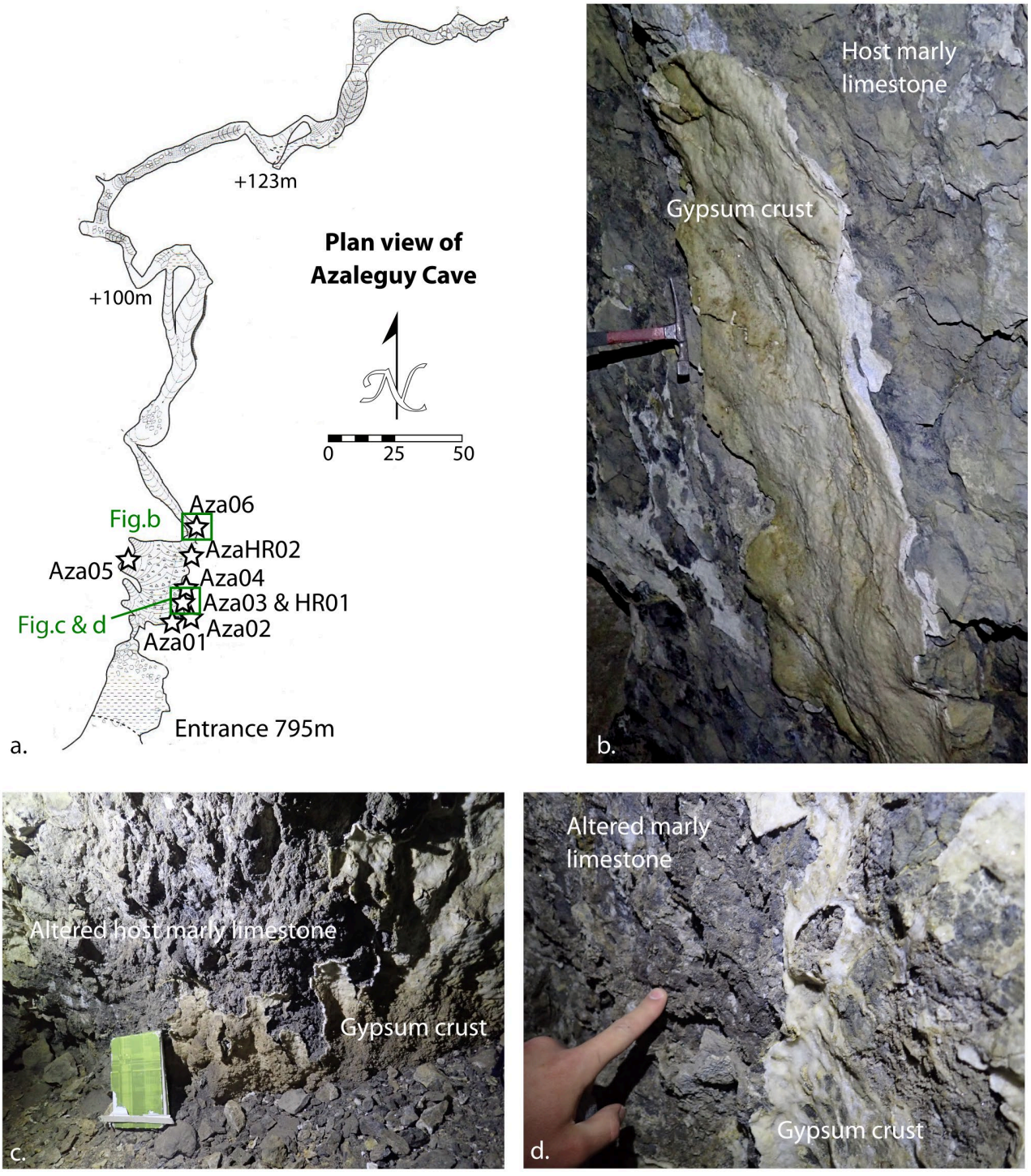

Figure S2: The Azaleguy karstic network. a. Map of the Azaleguy karstic network (topography drew by E. de Valicourt; positive numbers correspond to the altimetry from the entrance) and location of samples. b. Pluri-cm-thick platings of gypsum resting on H_2S-rich Albian marls. c. and d. Thin crusts, crosses and blebs infilling cm-large dissolution craters in H_2S-rich marls.

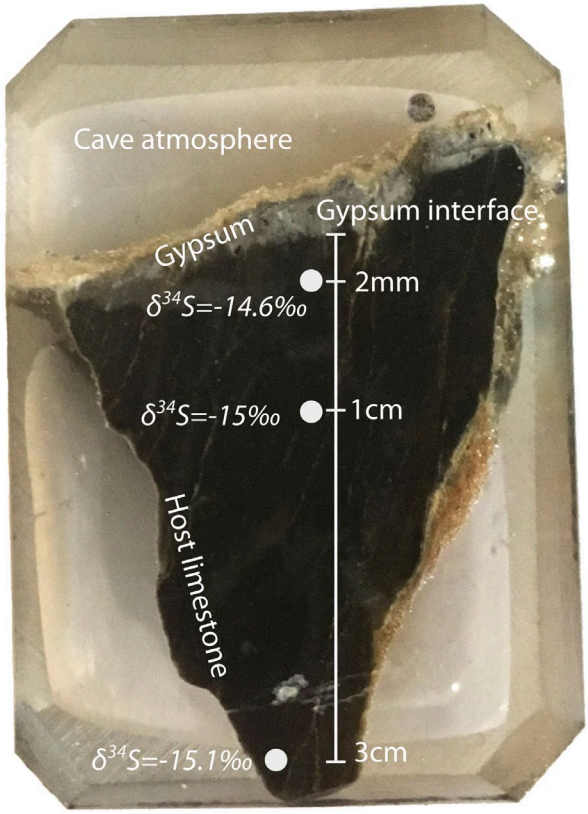

Figure S3: Down-rock sample profile for $\delta^{34}S$ measurements (in ‰ V-CDT) of trace sulfate minerals across a dissolution pocket in the Scrouitch gallery (see location in Supplementary Fig.1). Carbonate powder (samples NEBt) were sampled respectively at 2 mm, 1 cm and 3 cm from the gypsum-carbonate interface.

1.4. Notation of sulfur isotopy and calculation of mixing curves

All results of sulfur isotopes are reported in the classical delta notation with respect to Vienna Cañon Diablo Troilite (V-CDT):

$$\delta^{x}S = ({}^{x}R_{sample}/{}^{x}R_{reference} - 1) \times 1000 \quad (‰) \qquad (1)$$

with x = 33 and 34. To improve the analysed sample interpretations, and thus the determination of the involved process, we used the capital delta values defined as:

$$\Delta^{33}S = \delta^{33}S - 1000 \times [(1 + \delta^{34}S/1000)^{0.515} - 1] \qquad (‰) \qquad (2)$$

The standard deviation includes the internal and external errors possibly involved during extraction and fluorination procedure, and is better than 0.1‰ and 0.01‰ for $\delta^{34}S$ and $\Delta^{33}S$ values respectively.

In this study, we highlighted the presence of both thermochemical H_2S (TSR-derived H_2S) and microbial H_2S (MSR-derived H_2S) (see explanation in the main article). In order to evaluate the respective impact of TSR-derived and MSR-derived H_2S on cave sulfate mineral precipitation, we calculated a two components mixing curves between the MSR pole, defined from the signature of the dissolved H_2S in the Mainaltea spring, and the TSR pole, corresponding to the H_2S trapped within the cave host rock, using the following equation:

$$\left(\frac{\delta^{x}S_{mix}}{1000}+1\right)=\left(\frac{\delta^{x}S_{BSR}}{1000}+1\right)\times\chi_{BSR}+\left(\frac{\delta^{x}S_{TSR}}{1000}+1\right)\times\chi_{TSR} \quad (3)$$

where x = 33 or 34 and χ corresponds to the respective proportion of MSR-derived and TSR-derived H_2S (between 0 and 1).

Major sulfur isotopes of trace sulfate minerals in carbonate rocks

For trace sulfate minerals in limestones, about 10 mg of carbonate powder were weighed and cleaned. Samples stayed overnight in 3 ml of 10 wt% NaCl with 30 min ultrasonication at the beginning and at the end of the night. Samples were then centrifugated and rinsed three times in ultrapure water brought to a pH of 8 using ammonia and centrifugation. Samples were afterwards dissolved using 10% HCl for 30 min to 1h, centrifugated and dried down. The dry residue is then dissolved in 1 ml of ultrapure water, an aliquot of 20 to 50 µl was diluted in 0.2 to 1 ml of ultrapure water for measuring the sulfate concentration of the sample on a Metrohm ion chromatography system (ICS) and the rest was used for measuring isotopic composition. To purify the samples before analysis, we ran the samples on 0.8 ml of anionic resin Biorad AG1X8 100-200 mesh (Paris et al., 2014). Samples were analysed then on the ThermoScientific Neptune Plus MC-ICPMS at the Centre de Recherches Pétrographiques et Géochimiques (CRPG; Vandoeuvre-lès-Nancy, France) using a standard-sample bracketing method (Paris et al., 2013). Samples were run at high resolution using an Aridus-II desolvating membrane to decrease oxide and hydride interferences. Data are then corrected for instrumental fractionation, drift and background following Paris et al. (2013). The in-house bracketing Na_2SO_4 solution has been calibrated against international standard IAEA S1 and checked against IAEA S2 and S3. Seawater samples ran during each Neptune sessions to ensure accuracy of the measurement. All acids (except the acids used to clean the resin before sample introduction) are distilled at CRPG and ultrapure water is produced on a Helga system (Veolia, >18.2 MΩ resistivity). Errors (2sd) are estimated at ±0.2 ‰ for trace sulfate minerals based on long-term consistency standards.

Multiple sulfur isotopy (MSI) of cave sulfate minerals, sulfide minerals and dissolved sulfate/sulfide ions in springs

Determination of the total H_2S concentration trapped within a carbonate rock was performed on-line using the Thermo Scientific EA IsoLink IRMS System at CRPG. Millimetre size samples were wrapped in tin capsules (c.a. 40 mg) and then combusted at 1020 °C in a combustion reactor consisting of quartz tubes filled with chromium oxide, pure copper and silvered cobalt oxide. Produced gases (N_2, CO_2 and SO_2) were separated on a chromatographic column maintained at 70 °C. At this temperature, SO_2 was trapped inside the chromatographic column while N_2 and CO_2 were released. Five aliquots of the sample were successively measured following this procedure, that lead the accumulation of SO_2 into the chromatographic column. After this purification, the chromatographic column was heated to 240 °C. The produced SO_2 was then liberated, and the sulfur content was measured with a Thermo Scientific Delta V Advantage continuous flow isotope ratio mass spectrometer.

Multiple sulfur isotope analyses (^{32}S, ^{33}S, ^{34}S) were performed on powder from different samples:

(i) minerals of calcium and sodium sulfate from the Nébélé Cave, gypsum from Azaleguy Cave, evaporitic gypsum from Caresse quarry, and pyrites and pyrrhotites from the Cretaceous and Lias formations. These minerals were separated and reduced into the purest powder as possible;

(ii) spring waters of Uthurbietta, Camou and Mainaltea (Fig.1a in the main text for location). A solution of cadmium acetate ($Cd(CH_3COO)_2$) and of barium chloride ($BaCl_2$; concentration 0.1 mol/l) after filtration were directly added into the samples, to precipitate, respectively, sulfide ions as CdS and sulfate ions as $BaSO_4$;

(iii) H_2S trapped into the porosity of the Jurassic host rock was released after dissolution with a 12N HCl solution. The released H_2S was then carried by a N_2 flux to a solution of $AgNO_3$ to precipitate as Ag_2S.

All samples were transformed into Ag_2S before MSI analyses. Sulfur extraction from each powder was performed by a Chromium Reduced Sulfide (CRS) solution based on the study of Canfield et al. (1986) for sulfides, and by a Strongly Reducing Hydriodic Hypophosphorous acid solution (STRIP) as described in Kitayama et al. (2017) to extract sulfate. Finally, a step of fluorination and purification by cryogenic traps and gas chromatography converted all the Ag_2S into SF_6 which was then analysed on a ThermoFinnigan MAT 253 dual-inlet gas-source mass spectrometer. All extractions and fluorination steps were carried out at Institut de Physique du Globe de Paris (IPGP, France).

1.5. Strontium isotopy of cave sulfate and carbonate minerals

Strontium isotopes were measured at Institut Universitaire Européen de la Mer (IUEM; Plouzané, France) on 2 cave gypsums and 2 sodium sulfate minerals in the Nébélé Cave, and 4 cave gypsums and 2 host H_2S-rich carbonate rocks of the Azaleguy Cave. About 50 to 100 mg of powdered samples were weighed and dissolved in savillex beakers in acetic acid 30% for 24h at 100 °C on a hot plate. After centrifugation and evaporation to dryness, dry residues were taken

up into 1 ml of HNO_3 1M and centrifuged before loading on Biorad® columns using Eichrom® Sr-SPEC resin (Pin and Zalduegui, 1997). Sr was eluted in 2 ml of hot ultrapure H_2O. Samples were then loaded on W filaments and Sr isotope compositions were measured in static mode on a Thermo TRITON at the PSO (Pôle de Spectrométrie Océan) in Brest (France). All measured Sr ratios were normalized to $^{86}Sr/^{88}Sr = 0.1194$. During the analysis, Sr isotope compositions of standard solution NBS987 gave $^{87}Sr/^{86}Sr = 0.710270 \pm 0.000004$ (2σ, n=7, recommended value 0.710250).

1.6. Oxygen isotopy of cave sulfate minerals

Oxygen isotopic compositions of 3 gypsum and 3 sodium sulfate samples from the Nébélé Cave were measured at the Scientific and Technical Centers of the Universitat de Barcelona. Samples were weighed inside individual Ag boats to obtain 0.180 mg with a micro balance Mettler Toledo MX5. Samples were then wrapped and loaded into an autosampler coupled to TC/EA and Isotopic Relation Mass Spectrometry (IRMS) Delta plus xp Thermofisher for the isotopic composition measurement at a combustion temperature of 1450 °C. We used in this paper the classical delta notation in ‰ with respect to V-SMOW (mean ocean water) according to the equation:

$$\delta^{18}O = [(^{18}O/^{16}O)_{sample} /(^{18}O/^{16}O)_{V\text{-}SMOW}\text{-}1]*1000 \quad (4)$$

The reference standards used were NBS-127 ($\delta^{18}O$ value of +8.59 ‰), UB-ASC ($\delta^{18}O$ value of +13.2 ‰), UB-YCEM ($\delta^{18}O$ value of +17.6 ‰) and IAEA-SO6 ($\delta^{18}O$ value of -11.4 ‰) for an obtained standard deviation inferior to 0.2 ‰.

Table S1. Synthesis of isotopic analyses

Minerals/ water	Samples	$\delta^{34}S$ (‰ V-CDT)	Error	$\Delta^{33}S$ (‰)	Error	$^{87}Sr/^{86}Sr$	Error	$\delta^{18}O$ (‰ VSMOW)	Error
Nébélé Cave									
Gypsum	NEB01	-25.11	0.012	+0.009	0.008	0.700757	0.000004	+14.5	<0.2
	NEB02	-26.44	0.008	-0.009	0.008	0.708200	0.000004	+15.6	<0.2
	NEB03	-20.42	0.02					+10.3	<0.2
	NEB04	-20.20	0.02						
Thenardite/ Mirabilite	NEB05	-18.69	0.006	-0.002	0.010	0.707839	000004	+10.1	<0.2
	NEB06	-18.70	0.02					+10.5	<0.2
	NEB07	-19.43	0.02						
	NEB08	-21.98	0.014	-0.002	0.014	0.708071	000004	+10.5	<0.2
Host rock (limestone) H_2S in porosity	NEBe1	+13.29	0.005	+0.018	0.014				
	NEBn1	+15.93	0.017	-0.002	0.012				
	NEBn2	+15.81	0.013	+0.013	0.013				
	NEBn3	+16.29	0.01	+0.012	0.016				
Host rock (limestone) Trace sulfates	NEBt 2mm*	-14.60	0.2						
	NEBt 1cm*	-15.00	0.2						
	NEBt 3cm*	-15.10	0.2						
Uthurbietta Spring	Sulfates	+9.64	0.018	-0.031	0.022				
Azaleguy Cave									
Gypsum	Aza01	-19.60	0.007	-0.046	0.009	0.707307	0.000006		
	Aza02	-21.59	0.025	-0.024	0.012	0.707287	0.000004		
	Aza03	-21.82	0.017	-0.049	0.013	0.707290	0.000009		

Minerals/ water	Samples	$\delta^{34}S$ (‰ V-CDT)	Error	$\Delta^{33}S$ (‰)	Error	$^{87}Sr/^{86}Sr$	Error	$\delta^{18}O$ (‰ VSMOW)	Error
Gypsum	Aza04 Aza05 Aza06	-34.82 -20.68 -21.56	0.005 0.011 0.025	+0.040 -0.037 -0.049	0.008 0.012 0.012	0.707328	0.000006		
Host rock (limestone)	AzaHR01 AzaHR02					0.707273 0.707297	0.000006 0.000006		
Thermo-mineral springs									
Camou spring	Sulfates H_2S*	+14.55 +11.5	0.009 0.2	-0.046	0.012				
Mainaltea spring	Sulfates* H_2S In summer In winter	+0.9 -45.55 -53.90 -54.35	0.2 0.008 0.004 0.006	 +0.12 +0.179 +0.192	 0.012 0.008 0.009				
In sedimentary formations									
Triassic evaporite		+16.61	0.006	+0.003	0.016				
Sulfide minerals	Aptian pyrite	+0.98	0.011	-0.005	0.01				
	Aptian pyrrhotite	+3.89 +3.59	0.016 0.016	-0.004 -0.005	0.01 0.01				
	Liassic pyrite	-2.18	0.01	+0.162	0.01				

2

Note: All the sample marked by a star * have been measured for sulfur isotopy using the ThermoScientific Neptune Plus MC-ICPMS, while the other samples were analysed by a ThermoFinnigan MAT 253 dual-inlet mass spectrometer.

2. Additional information on the CO2 budget calculation

MSI interpretation revealed that at least 94% of sulfate ions currently dissolved in the karstic water of the Nebele Cave derives from the oxidation of the fossil TSR-derived H2S. It is known that calcite dissolution by 1 mole of sulfuric acid (H2SO4) releases 2 moles of carbon as bicarbonate ions (HCO3 -) (equation (5)):

2CaCO3(calcite) + H2SO4 → 2Ca2+ + 2HCO3 - + SO4 2- (5)

Then, as karstic groundwater is connected to surface water, this carbon is conveyed up to the river and the ocean with a climatic implication as half of the bicarbonate ions is released into the atmosphere as CO2 during calcite precipitation (equation (6)):

Ca2+ + 2HCO3 - → CaCO3(calcite) + CO2(gas) + H2O (6)

We considered a total volume of the currently active karstic part of the Nebele Cave of 234 910 m3 (calculated from the 3D topography provided by the Collectif Nebele). Then, for the budget calculation, we used a content of bicarbonate ions of 159 mg/l and a sulfate ions concentration of 18.4 mg/l in the water (Vanara, 2000). As this karstic volume is initiated 406.9 (+78.7/-46.6) kyr ago (Pleistocene uplift; obtained from palaeomagnetism and U/Th dating on speleothems in Vanara, 2000), the CO2 rate (considering a constant dissolution rate), only linked to the dissolution of carbonate rock by the oxidation of H2S trapped within porosity, is 9.5 g/yr, when the total CO2 rate is 66.2 g/yr (calculated from the current bicarbonate concentration).

For the CO2 budget calculation at the scale of the whole Arbailles karstic massif, we considered a total area of 185 km2, a mean thickness of Jurassic formation of 200 m, and that SAS affects all of the Jurassic limestone uniformly. Considering a current specific dissolution rate of 94 m3/km2/yr (Vanara, 2000), 19% of the total volume of Jurassic limestones can be karstified during the last 407 kyr in the Arbailles massif. With the same mean concentration of dissolved sulfate ions as for the Nebele Cave resurgence (18.4 mg/l), this karstified volume can produced at least 0.29t CO2/yr just from the H2S trapped in porosity since the major Pleistocene uplift. In addition, MSI

12

177

178

40 179
41 180
42 181
43 182
44 183
45 184
46 185
47 186
48 187
49 188
50 189
51 190
52 191
53 192
54 193
55 194
56 195
57 196
58 197
59 198
60 199
61 200
62 201
63 202
64
65
66
67
68
69
70
71

References

Canfield, D. E., Raiswell, R., Westrich, J. T., Reaves, C. M., and Berner, R. A., 1986, The use of chromium reduction in the analysis of reduced inorganic sulfur in sediments and shales: Chemical geology, 54(1-2), p. 149-155.

Kitayama, Y., Thomassot, E., Galy, A., Golovin, A., Korsakov, A., d'Eyrames, E., Assayag, N., Bouden, N., and Ionov, D., 2017, Co-magmatic sulfides and sulfates in the Udachnaya-East pipe (Siberia): A record of the redox state and isotopic composition of sulfur in kimberlites and their mantle sources: Chemical Geology, 455, p. 315-330.

Paris, G., Adkins, J. F., Sessions, A. L., Webb, S. M., and Fischer, W. W., 2014, Neoarchean carbonate–associated sulfate records positive Δ33S anomalies: Science, 346 (6210), p. 739-741.

Paris, G., Sessions, A. L., Subhas, A. V., and Adkins, J. F., 2013, MC-ICP-MS measurement of δ34S and Δ33S in small amounts of dissolved sulfate: Chemical Geology, 345, p. 50-61.

Pin, C., and Zalduegui, J. S., 1997, Sequential separation of light rare-earth elements, thorium and uranium by miniaturized extraction chromatography: application to isotopic analyses of silicate rocks: Analytica Chimica Acta, 339(1-2), p. 79-89.

Vanara, N., 2000, Le karst des Arbailles (Pyrenees-Atlantiques, France): Karstologia, 36(1), 23-42.

3. Additional information on the CO_2 budget calculation

MSI interpretation revealed that at least 94% of sulfate ions currently dissolved in the karstic water of the Nébélé Cave derives from the oxidation of the fossil TSR-derived H_2S. It is known that calcite dissolution by 1 mole of sulfuric acid (H_2SO_4) releases 2 moles of carbon as bicarbonate ions (HCO_3^-) (equation (5)):

$$2CaCO_{3(calcite)} + H_2SO4 \rightarrow 2Ca^{2+} + 2HCO_3^- + SO_4^{2-} \quad (5)$$

Then, as karstic groundwater is connected to surface water, this carbon is conveyed up to the river and the ocean with a climatic implication as half of the bicarbonate ions is released into the atmosphere as CO_2 during calcite precipitation (equation (6)):

$$Ca^{2+} + 2HCO_3^- \rightarrow CaCO_{3(calcite)} + CO_{2(gas)} + H_2O \quad (6)$$

We considered a total volume of the currently active karstic part of the Nébélé Cave of 234 910 m^3 (calculated from the 3D topography provided by the Collectif Nébélé). Then, for the budget calculation, we used a content of bicarbonate ions of 159 mg/l and a sulfate ions concentration of 18.4 mg/l in the water (Vanara, 2000). As this karstic volume is initiated 406.9 (+78.7/-46.6) kyr ago (Pleistocene uplift; obtained from palaeomagnetism and U/Th dating on speleothems in Vanara, 2000), the CO_2 rate (considering a constant dissolution rate), only linked to the dissolution of carbonate rock by the oxidation of H_2S trapped within porosity, is 9.5 g/yr, when the total CO_2 rate is 66.2 g/yr (calculated from the current bicarbonate concentration).

For the CO_2 budget calculation at the scale of the whole Arbailles karstic massif, we considered a total area of 185 km^2, a mean thickness of Jurassic formation of 200 m, and that SAS affects all of the Jurassic limestone uniformly. Considering a current specific dissolution rate of 94 $m^3/km^2/yr$ (Vanara, 2000), 19% of the total volume of Jurassic limestones can be karstified during the last 407 kyr in the Arbailles massif. With the same mean concentration of dissolved sulfate ions as for the Nébélé Cave resurgence (18.4 mg/l), this karstified volume can produced at least 0.29t CO_2/yr just from the H_2S trapped in porosity since the major Pleistocene uplift. In addition, MSI interpretation reveals that microbial influence on the Nébélé Cave development is predominant during the progressive dewatering of galleries, with a relative influence of 59% against 41% for the trapped TSR-derived H_2S. Considering the influence of both MSR-derived and TSR-derived H_2S, the CO_2 rate during the sulfuric acid dissolution of Jurassic formations is of 0.7t CO_2/yr in the Arbailles massif.

Finally, for the CO_2 rate calculation linked to the TSR-derived H_2S at the scale of South Aquitaine Basin and northern Pyrenean foothills, we took a total area of 9000 km^2 for a constant thickness of the Jurassic formations of 200 m. Then using the same karstification potential of 19% estimated for the Arbailles massif during the last 407 kyr, and the same concentration of dissolved sulfate ions, we obtained a carbon budget of 13.9 t CO_2/yr, only linked to the trapped TSR-derived H_2S. The CO_2 rate is therefore higher if we take into account the microbial influence on sulfuric acid dissolution with a total carbon budget of 33.9 t CO_2/yr.

References

Canfield, D. E., Raiswell, R., Westrich, J. T., Reaves, C. M., and Berner, R. A., 1986, The use of chromium reduction in the analysis of reduced inorganic sulfur in sediments and shales: Chemical geology, 54(1-2), p. 149-155.

Kitayama, Y., Thomassot, E., Galy, A., Golovin, A., Korsakov, A., d'Eyrames, E., Assayag, N., Bouden, N., and Ionov, D., 2017, Co-magmatic sulfides and sulfates in the Udachnaya-East pipe (Siberia): A record of the redox state and isotopic composition of sulfur in kimberlites and their mantle sources: Chemical Geology, 455, p. 315-330.

Paris, G., Adkins, J. F., Sessions, A. L., Webb, S. M., and Fischer, W. W., 2014, Neoarchean carbonate–associated sulfate records positive Δ33S anomalies: Science, 346 (6210), p. 739-741.

Paris, G., Sessions, A. L., Subhas, A. V., and Adkins, J. F., 2013, MC-ICP-MS measurement of δ34S and Δ33S in small amounts of dissolved sulfate: Chemical Geology, 345, p. 50-61.

Pin, C., and Zalduegui, J. S., 1997, Sequential separation of light rare-earth elements, thorium and uranium by miniaturized extraction chromatography: application to isotopic analyses of silicate rocks: Analytica Chimica Acta, 339(1-2), p. 79-89.

Vanara, N., 2000, Le karst des Arbailles (Pyrénées-Atlantiques, France): Karstologia, 36(1), 23-42.